Pamukkale Univ Muh Bilim Derg, 31(8), 1505-1517, 2025
(Special Issue of the 10th Geochemistry Symposium)

Pamukkale Üniversitesi Mühendislik Bilimleri Dergisi

Pamukkale University Journal of Engineering Sciences

Mineral chemistry of isotropic gabbro and plagiogranite from the Central Anatolian Ophiolites in the Derinkuyu (Nevşehir, Central Anatolia) region

Derinkuyu (Nevşehir, Orta Anadolu) yöresindeki Orta Anadolu Ofiyolitlerinden izotropik gabro ve plajiyogranitin mineral kimyası

Ayşe Orhan[1*], *Musa Avni Akçe*[1]

[1]Department of Geological Engineering, Faculty of Engineering and Architecture, Nevşehir Hacı Bektaş Veli Univ., Nevşehir, Türkiye.
ayse.orhan@nevsehir.edu.tr, akce@nevsehir.edu.tr

Received/Geliş Tarihi: 16.10.2025 Revision/Düzeltme Tarihi: 06.11.2025 doi: 10.65206/pajes.63504
Accepted/Kabul Tarihi: 11.11.2025 Special Issue Article/Özel Sayı Makalesi

Abstract

The isotropic gabbro and plagiogranite belonging to the Central Anatolian Ophiolites, are exposed as stocks around Derinkuyu (Nevşehir). Plagiogranite, which cuts the isotropic gabbro, contains mafic microgranular enclaves (MME) belonging to these rocks. Gabbro and MME contain plagioclase, clinopyroxene and hornblende minerals. The isotropic gabbros are in hornblende-pyroxene and pyroxene-hornblende/hornblende gabbro compositions. Plagiogranite is composed of quartz, plagioclase and hornblende, and exhibits a tonalite composition. Mineral chemistry analysis results indicate that plagioclases in the gabbro, plagiogranite, and MME have compositions of andesine–bytownite ($An_{47–85}$), andesine ($An_{38–48}$), and labradorite–bytownite ($An_{65–75}$), respectively. Clinopyroxenes (Mg#=0.73–0.84) and hornblendes (Mg#=0.57–0.79) are characterized by their high-Mg contents. Clinopyroxenes, diopside–augite ($En_{37–43}Fs_{12–15}Wo_{42–47}$), and the hornblendes exhibit compositions of tschermakite–magnesio-hornblende. Clinopyroxene and hornblende data on the discrimination diagrams indicate the presence of an island arc for the source magma. Pyroxene and amphibole thermobarometry suggest that P–T crystallization conditions for clinopyroxene and hornblende 2.60–1.37 kbar 1199–1186°C and 1.95–1.09 kbar; 864–790°C, respectively. These data manifest that the magma of supra-subduction type ophiolite rise towards shallow lithospheric levels (9.2–3.9 km).

Keywords: Isotropic gabbro, Plagiogranite, Mineral chemistry, Supra-subduction zone, Central Anatolia.

Öz

Orta Anadolu Ofiyolitlerine ait izotropik gabro ve plajiyogranitler, Derinkuyu (Nevşehir) çevresinde stoklar halinde yüzeylemektedir. İzotropik gabroyu kesen plajiyogranit, bu kayaçlara ait mafik mikrogranüler anklavları (MME) içerir. Gabro ve MME plajiyoklaz, klinopiroksen ve hornblend mineralleri içerir. İzotropik gabrolar, hornblend-piroksen ve piroksen-hornblend/hornblend gabro bileşimlerindedir. Plajiyogranit, kuvars, plajiyoklaz ve hornblendden oluşur ve tonalit bileşimi gösterir. Mineral kimyası analiz sonuçları, gabro, plajiyogranit ve MME'deki plajiyoklazların sırasıyla andezin–bitovnit ($An_{47–85}$), andezin ($An_{38–48}$) ve labradorit–bitovnit ($An_{65–75}$) bileşimlerine sahip olduğunu göstermiştir. Klinopiroksen (Mg#=0.73–0.84) ve hornblendler (Mg#=0.57–0.79) yüksek-Mg içerikleriyle karakteristiktir. Klinopiroksenler, diyopsit–ojit ($En_{37–43}Fs_{12–15}Wo_{42–47}$) ve hornblendler çermakit–magnezyum-hornblend bileşimleri sergiler. Sınıflama diyagramlarında klinopiroksen ve hornblend verileri, kaynak magma için bir ada yayının varlığını göstermektedir. Piroksen ve amfibol termobarometrisi, klinopiroksen ve hornblend için P-T kristalleşme koşullarının sırasıyla 2.60–1.37 kbar; 1199–1186°C ve 1.95–1.09 kbar; 864–790°C olduğunu göstermektedir. Bu veriler, dalma-batma zonu üstü tipi ofiyolit magmasının sığ litosferik seviyelere (9.2–3.9 km) doğru yükseldiğini ortaya koymaktadır.

Anahtar kelimeler: İzotropik gabro, Plajiyogranit, Mineral kimyası, Dalma-batma zonu üstü, Orta Anadolu.

1 Introduction

Ophiolites formed in different tectonic environments are generally classified as mid-ocean ridge (MORB)-type and Supra-Subduction Zone (SSZ)-type [1]. SSZ-type ophiolites are thought to have formed as a result of partial melting of the upper mantle+oceanic lithosphere wedged directly onto the subducting oceanic plate [1],[2]. In SSZ-type ophiolites, generally clinopyroxene and sometimes orthopyroxene crystallize before plagioclase, while in MORB-type ophiolites the opposite is true [1]. Therefore, in SSZ-type ophiolites, cumulate dunite, lherzolite, wehrlite, norite, and gabbro formations follow from the base upwards [1]. Another important feature of SSZ-type ophiolites is the high proportion of low-K, high-SiO_2 leucocratic bodies, defined as oceanic plagiogranite [3], in their upper levels [1],[4]. SSZ-type ophiolite minerals are characterized by Mg-rich olivine, clinopyroxene, amphibole, and Ca-rich plagioclase compositions [5]-[13].

The study area is located within the Central Anatolian Crystalline Complex (CACC) (Figure 1a, b) [14],[15]. Ophiolitic bodies exposed south of the İzmir–Ankara–Erzincan Suture Zone (IAESZ) within the CACC are named as Central Anatolian Ophiolites (CAO) (Figure 1b) [16]. Geochemical and isotopic data from the CAO indicate that these ophiolites formed in the supra-subduction zone (SSZ-type) fore-arc basin within the Neo-Tethyan ocean [4]-[7],[13],[17]-[21]. Evidence for the SSZ-type ophiolite formation in the CAO is not limited solely to whole-rock geochemical data. The clinopyroxene and plagioclase compositions in the ophiolites show high Mg, low Ti, and high anorthite content, similar to SSZ-type Eastern Mediterranean ophiolites [5]-[7],[13].

*Corresponding author/Yazışılan Yazar

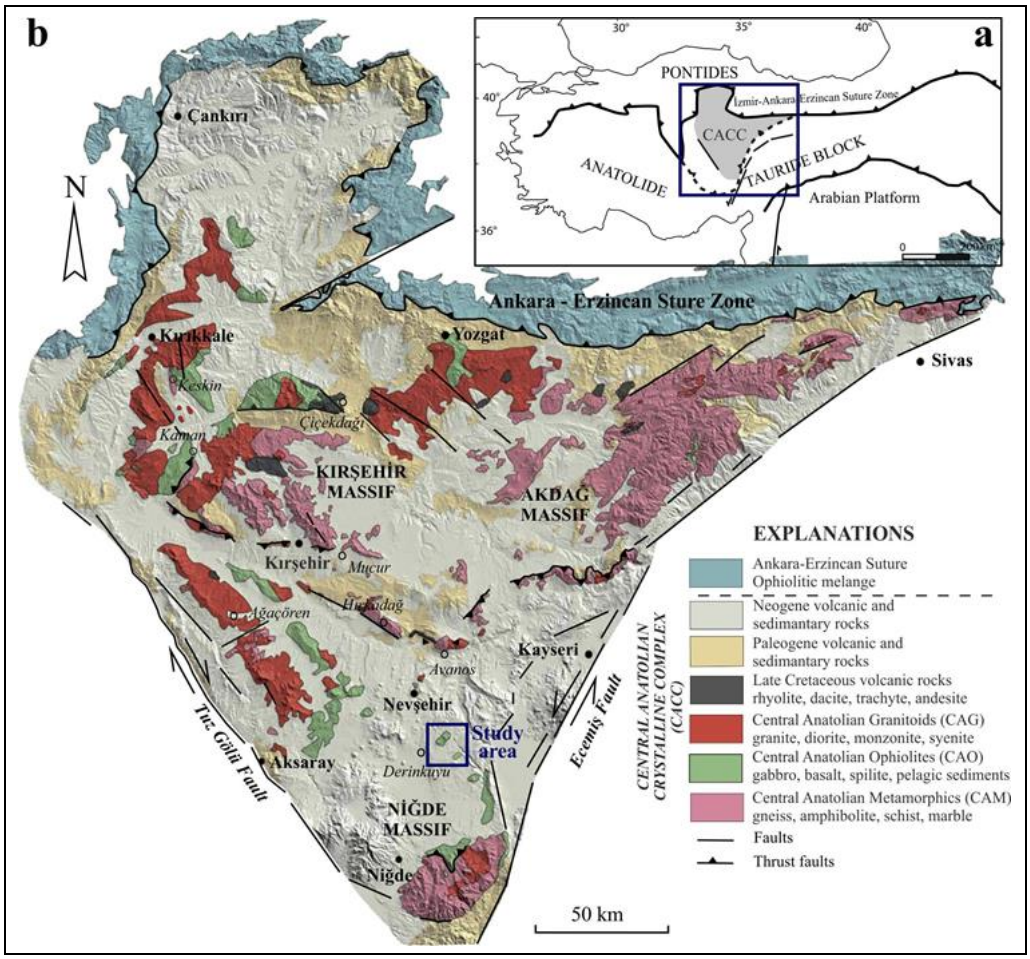

Figure 1. (a): Tectonic terrane map of Türkiye (simplified from Okay and Tüysüz [14]). (b): Regional geological map of the Central Anatolian Crystalline Complex (CACC) (modified from Lefebvre et al. [15]).

The isotropic gabbro and plagiogranite belonging to the CAO, which constitute the subject of the study, are exposed in the form of stocks around Derinkuyu (Nevşehir) (Figure 1b and Fgiure 2). In previous studies, the gabbro and plagiogranite rocks in the vicinity of Aksaray–Kayseri, including the study area, were identified mineralogically and petrographically [23]. According to geochemical data, these rocks may have derived from a MORB-like source [23]. Although whole-rock geochemical studies have been conducted on the rocks in the study area, mineral chemistry data are not available. In this study, the petrographic characterization and mineral chemistry results of CAO rocks around the Derinkuyu region are presented together. Deficiencies in the literature have been eliminated with mineral chemistry data, and the petrogenetic evolution and crystallization conditions of ophiolitic rocks in this region have been investigated.

2 Geological setting and field relation

Türkiye is part of the Alpine–Himalayan orogenic belt, which is characterized by several continental fragments and suture zones (Figure 1a) [14]. The CACC is a triangular area bounded by the IAESZ to the north, the Anatolide–Tauride platform to the south, the Salt Lake Fault to the west, and the Ecemiş Fault to the east (Figure 1b) [15],[16]. The Complex consists mainly of Central Anatolian Metamorphic (CAM), Central Anatolian Ophiolitic (CAO), and Central Anatolian Granitic (CAG) rocks, which are covered by Cenozoic sedimentary and volcano-sedimentary rocks [15],[16]. The CAM, which forms the basis of the CACC, indicates that regional metamorphism developed in two stages: high-amphibolite–granulite facies and greenschist facies [15],[24],[25]. U/Pb dating on monazite and zircon from the high amphibolite facies determined the age of metamorphism as ~91–84 Ma [26],[27].

The CAO, which is the remnants of the northern branch of the Neo-Tethyan Ocean and forms the basis of the study area, tectonically overlies the metamorphics. The CAO exhibits the geochemical features of typical SSZ-type ophiolites [4]-[7],[13],[17]-[21]. The CAO bodies are mostly fragmented, but the ophiolitic sequence is preserved in some locations [4],[17],[18].

The SSZ-type ophiolitic sequence is represented by metamorphic tectonites, cumulate and isotropic gabbro, plagiogranite, diabase of the sheeted dyke complex, pillow lava, and deep-sea sediments [4],[18]. SSZ-type ophiolite magma was derived from a depleted magma source modified by a subduction component [21]. U/Pb dating on zircon in gabbro and plagiogranite determined the crystallization age of these rocks as 94.9 Ma [13] and 90.5 Ma [28].

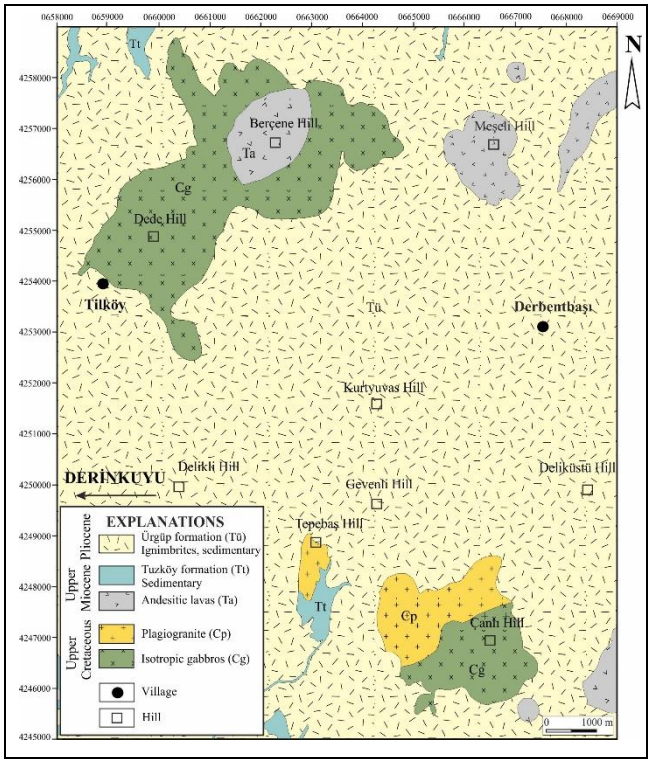

Figure 2. Geological map of the study area [22].

In the CACC, widespread magmatism (CAG) events developed shortly after the obduction of SSZ-type ophiolites onto the CAM. The CAG intruded the region by cutting the CAM and/or CAO rocks and has a wide compositional range [29]-[35]. This magmatism, which lasted approximately 20 Ma (95–74 Ma; [36],[37]), is represented by calc-alkaline to alkaline affinity and I-S-type, I-/H-type, and A-type compositions.

The study area is located northeast and east of Derinkuyu (Nevşehir), where igneous rocks of the CAO are exposed in small stocks (Figure 2) [22],[38]. This unit is covered by Upper Miocene–Pliocene pyroclastic rocks belonging to the Cappadocia Volcanic Province and sedimentary rocks. It has been stated that the ophiolite sequence in the region does not present a complete sequence [38]. Isotropic gabbro is the dominant rock type of the CAO around Dede Hill, north of Tilköy (Figure 2). In this region, gabbro is dark-colored, coarse-grained, and is exposed at the upper levels of the elevations (Figure 3a). The isotropic gabbro is cut by diabase dykes with a fine-grained texture and a dark green color, varying in thickness from 0.5–1 m. The orientation of the dykes is N65W. Plagiogranite is exposed around Tepebaş Hill and Çanlı Hill (Figure 2). Around Çanlı Hill, isotropic gabbro is cut by plagiogranite (Figure 3b). Plagiogranite contains irregular shaped mafic microgranular enclaves (MME) of the isotropic gabbro. Gabbro is dark-colored, while plagiogranite is gray. Gabbro and plagiogranite are mostly medium- to coarse- and fine- to medium-crystalline. Enclaves with ellipsoidal shapes are fine-crystalline.

3 Samples and analytic methods

Thin sections of a total of 31 samples taken from gabbro and plagiogranite were prepared at the Mineral Research and Exploration General Directorate (MTA), and electron microprobe analyses (EPMA) of 4 samples were performed at

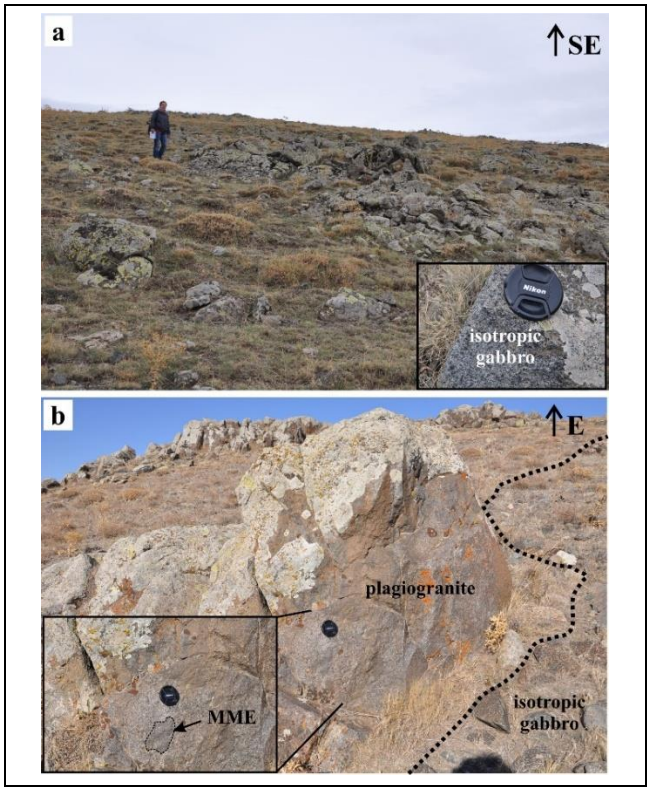

Figure 3. Field view (a): of isotropic gabbro around Tilköy, and (b): Gabbro and plagiogranite around Çanlı Hill.

the Ankara University Earth Sciences Application and Research Center.

Mineralogic-petrographic analyses were carried out using a Nikon 50iPOL polarizing microscope at the Department of Geological Engineering, Nevşehir Hacı Bektaş Veli University. Imaging of thin sections was performed with a 5-megapixel Nikon digital camera system connected to the same microscope. In addition, point counting (500 points) was performed on 23 thin-section samples using a PELCON automatic point counter and its associated software. Polished and carbon-coated thin sections were prepared before the mineral chemistry analysis. Electroprobe Micro Analyzer (EPMA) analyses were performed using the JEOL JXA–8230 electron microprobe equipped with 5 WDS detectors. For the calibration and measurements, natural oxide and mineral reference materials were used. The stoichiometric calculations of the minerals analyzed by EPMA were made based on 6 oxygens for pyroxene, 26 oxygens for amphibole, and 8 oxygens for plagioclase. The end-members of the minerals were calculated and shown in the diagrams. To estimate the crystallization conditions (P–T) of the rocks, the equations proposed by Wang et al. [39] and Ridolfi et al. [40] for pyroxene and amphibole were used.

4 Analytical results

4.1 Petrography

Petrographic features of isotropic gabbros, plagiogranites, and MMEs in the region are presented in Table 1. Isotropic gabbro is generally a medium- to coarse-grained and hypidiomorphic granular texture (Figure 4a–d). It consists of plagioclase, clinopyroxene, and hornblende as the main phenocrysts.

Table 1. Petrographic characteristics of isotropic gabbro, plagiogranite, and MMEs in the study area (Ap–Apatite; Bt–Biotite; Cpx–Clinopyroxene; Hbl–Hornblende; Pl–Plagioclase; Opq–Opaque; Qz–Quartz).

Area	Rock type	Grain size	Texture	Main minerals	Accessory minerals	Alteration minerals
Tilköy	Hornblende-pyroxene gabbro	Medium- to coarse	Hypidiomorphic, subophitic	Pl I ($An_{47–65}$) (45–55%) + Cpx (28–37%) + Hbl (9–16%)	Opq	Uralite, actinolite, chlorite, epidote ± albite
	Pyroxene-hornblende/ hornblende gabbro	Medium- to coarse	Hypidiomorphic	Pl II ($An_{69–85}$) (52–60%) + Hbl (21–44 %) + Cpx (1–17 %)	Opq	Uralite, chlorite, epidote
Çanlı Hill	Plagiogranite (tonalite)	Medium- to coarse	Hypidiomorphic	Pl II ($An_{38–48}$) (55–66 %) + Qz (20–32 %) + Hbl (10–13 %)	Bt, Cpx, Opq, Ap	Chlorite
	MME (Pyroxene-hornblende gabbro)	Fine	Hypidiomorphic	Pl II ($An_{65–75}$) (58–59 %) + Hbl (19–20 %) + Cpx (5–16 %)	Opq	Chlorite

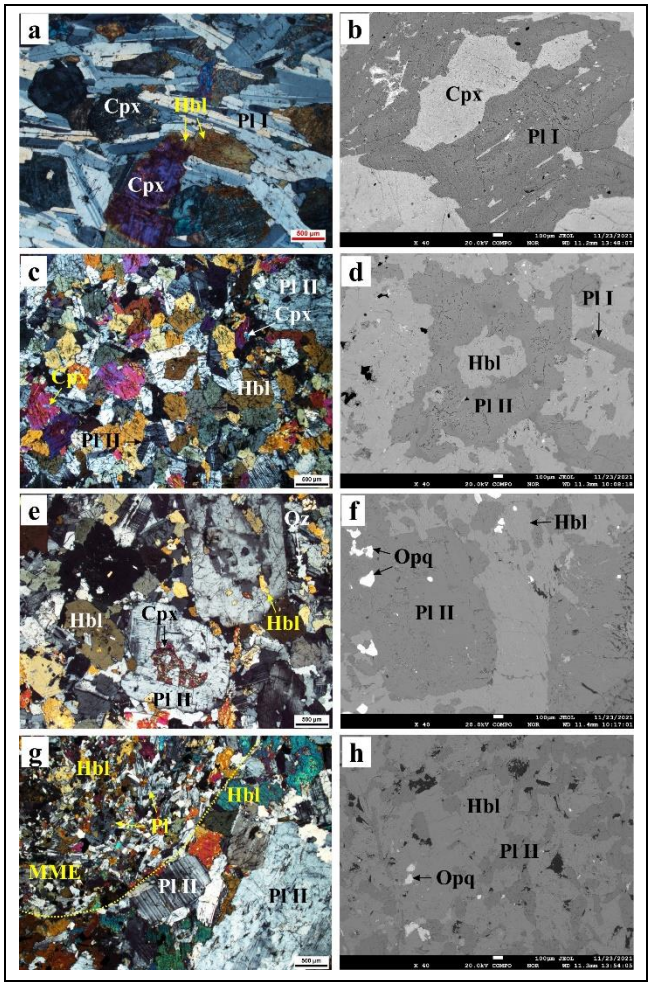

Figure 4. Photomicrographs (XPL) and BSE images of the investigated gabbro, plagiogranite and MME's. (a),(b): Sub-ophitic texture of intergrown plagioclase laths and clinopyroxene in the gabbro. (c),(d): Medium-grained and hipidiomorphic granular texture in the gabbro. (e),(f): Coarse-grained and hipidiomorphic granular texture in the plagiogranite. (g),(h): The contact between fine-grained MME and coarse-grained plagiogranite (Cpx–Clinopyroxene; Hbl–Hornblende; Pl–Plagioclase; Opq–Opaque; Qz–Quartz).

It contains secondary and accessory minerals such as actinolite, epidote, chlorite, and opaque minerals. Based on their mineral abundance, the gabbros around Tilköy and Çanlı Hill were identified as hornblende-pyroxene gabbro and pyroxene-hornblende/hornblende gabbro. (Table 1 and Figure 5b) [41]. Plagiogranite has a medium-coarse grained hypidiomorphic granular texture (Figure 4e, f). It is composed of plagioclase, quartz, and hornblende as the main minerals and does not contain K-feldspar (Table 1). Chlorite, biotite, clinopyroxene, apatite, and opaque minerals are observed as secondary and accessory minerals. Plagiogranites are in tonalite composition on the Streckeisen QAP diagram (Figure 5a)[41]. The MME is fine-grained and in sharp contact with the host rock (Figure 4g, h). It contains plagioclase, hornblende, and clinopyroxene as main phenocrysts, with minor amounts of opaque minerals (Table 1). MMEs plot into pyroxene-hornblende gabbro, like the isotropic gabbro in this region. (Figure 5b)[41].

Two types of plagioclase phenocrysts were identified within the isotropic gabbro. The first type (Pl I) exhibits euhedral and polysynthetic twinning in the form of laths (Figure 4a, b, d). Pl I is generally observed in the hornblende-pyroxene gabbro around Tilköy. These plagioclases are surrounded by pyroxene phenocrysts and exhibit a subophitic texture (Figure 4a, b). The second type of plagioclase (Pl II) is mostly observed in the pyroxene-hornblende/hornblende gabbro around Çanlı Hill. Pl II exhibits euhedral to subhedral and wavy extinctions (Figure 4c, d). Therefore, two generations of plagioclase formations may be specified. Pl II is accompanied by abundant hornblende and, to a lesser extent, pyroxene. Pyroxene and hornblende phenocrysts in gabbro samples vary from anhedral to euhedral. Pyroxenes have a green color and strong interference colors (Figure 4a, c) and are likely clinopyroxene. Hornblendes show pleochroism from green to brown. They were formed as a result of the uralitization of clinopyroxenes from their edges towards the center (Figure 4a, c). It can be said that hornblende developed as a result of magmatic uralitization during the crystallization of magma. Hornblendes are observed mostly together with Pl II in the pyroxene-hornblende/hornblende gabbro around Çanlı Hill (Figure 4c, d). It can be said that hornblende almost completely replaced clinopyroxene and gained its crystalline form. They are subhedral and euhedral in shape.

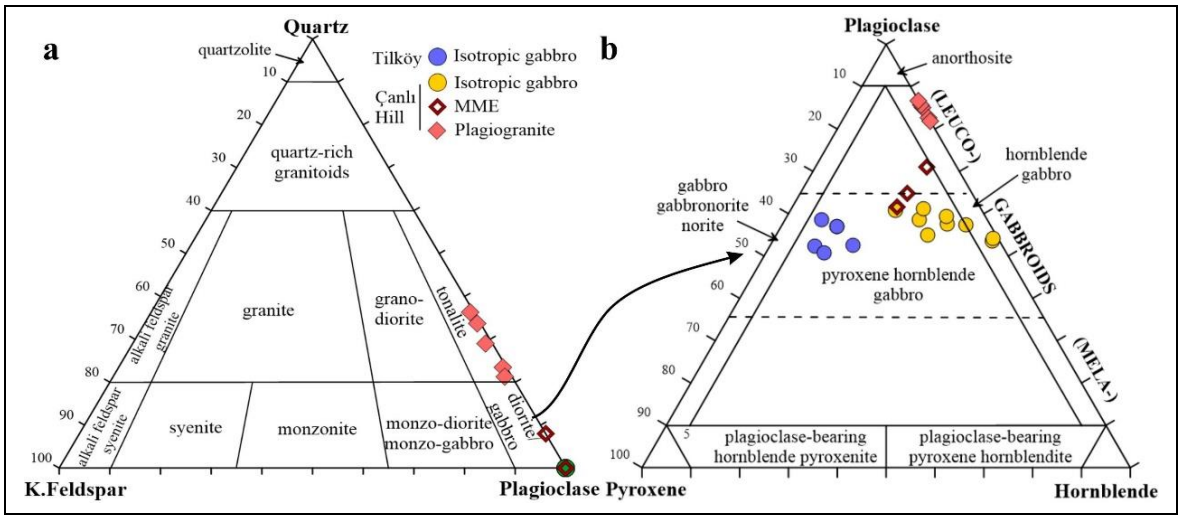

Figure 5. (a): Quartz–A.Feldspar–Plagioclase, and (b): Plagioclase–Pyroxene–Hornblende modal classification [41] for the isotropic gabbros, plagiogranites and MMEs around the Derinkuyu region.

According to textural features, it can be said that the crystallization order of gabbro is plagioclase (Pl I) + clinopyroxene → plagioclase (Pl II) + hornblende. The replacement of clinopyroxene by actinolite is a common phenomenon. Secondary actinolite is sometimes accompanied by chlorite. Actinolite is characterized by its green color and fibrous structure. Albitization and epidotization are observed in some plagioclase (Pl I).

Plagioclase grains (Pl II) in the plagiogranite, as in the isotropic gabbro around Çanlı Hill, are in the form of euhedral and subhedral phenocrysts (Figure 4e, f). It presents polysynthetic twinning, oscillatory zoning, and wavy extinctions. Zoned plagioclases contain clinopyroxene and hornblende inclusions. Some plagioclase-quartz intergrowths are also observed. Quartz is generally anhedral and fills the spaces between other minerals. Hornblende is the most observed ferromagnesian mineral. It is generally subhedral and euhedral. Some hornblendes contain fine-grained prismatic plagioclase and clinopyroxene inclusions. Biotite and chlorite formations on hornblende are rarely observed.

The MME has properties and mineralogy similar to those of pyroxene-hornblende gabbro in the region (Figure 4g, h). Plagioclase (Pl II) is euhedral and subhedral. It exhibits polysynthetic twinning and oscillatory zoning (Figure 4g). The zoned plagioclases contain clinopyroxene and hornblende inclusions. Hornblende is subhedral and euhedral.

4.2 Mineral chemistry

Mineral chemistry results of clinopyroxene, hornblende, and plagioclase minerals from the isotropic gabbro, MME, and plagiogranite from around the Derinkuyu are given in Appendix A, B, and C.

4.2.1 Clinopyroxene

Analysis results of clinopyroxenes in the investigated gabbro are presented in Appendix A and shown in Figure 6. Studied clinopyroxenes are characterized by high SiO_2 (50.01–51.71 wt.%), high MgO (12.67–14.67 wt.%), high CaO (19.88–22.42 wt.%), and low FeO (7.21–9.38 wt.%) contents. They have relatively high Mg# 0.73–0.84 (Mg# = (Mg/[Mg + Fe]), low Al_2O_3(1.11–2.50 wt.%) and TiO_2(0.14–0.76 wt.%) concentrations. Clinopyroxene compositions vary in a narrow range ($En_{37-43}Fs_{12-15}Wo_{42-47}$) and show diopside–augite compositions in the ternary classification diagram (Figure 6) [42].

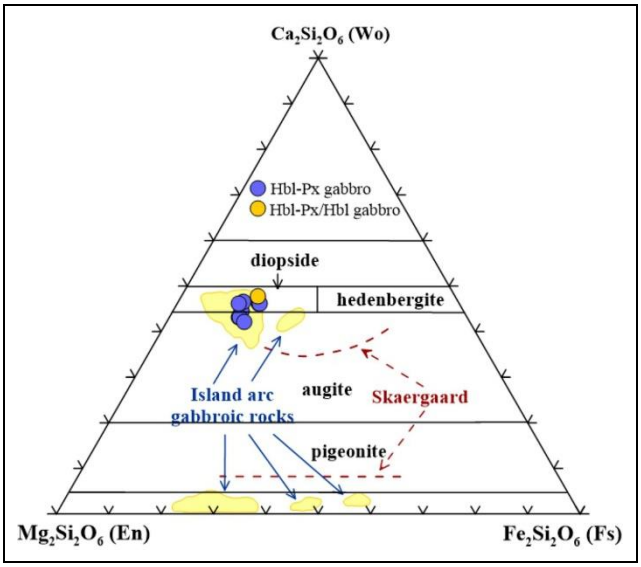

Figure 6. Ternary classification diagram showing compositional variation for clinopyroxenes in the isotropic gabbro [42] (the island arc gabbroic rock fields and Skaergaard trends are taken from Burns [43]).

4.2.2 Amphibole

EPMA results of amphiboles in the investigated rocks are presented in Appendix B. According to the analysis results, amphiboles show differences in major-element composition across the three rock types. Amphiboles in the isotropic gabbro have relatively low SiO_2 (42.73–46.40 wt.%) and high TiO_2 (0.85–1.73 wt.%), high Al_2O_3 (7.06–9.18 wt.%), and high Na_2O (0.88–1.54 wt.%) contents compared to those of plagiogranite and MEE. In the plagiogranite and MME, SiO_2 (51.17–51.93

wt.% and 44.80–46.71 wt.%) contents are high, while TiO_2 (0.57–0.88 wt.% and 0.52–1.16 wt.%), Al_2O_3 (6.67–7.33 wt.% and 6.94–8.43 wt.%), and Na_2O (0.74–0.85 wt.% and 0.93–1.05 wt.%) contents are relatively low. All amphiboles can be classified as "calcic amphiboles" according to (Ca+Na)>1.0 and CaB>1.5. (Appendix B) [44]. The Mg# (Mg/[Mg+Fe]) and atomic proportion of Si for amphiboles in the isotropic gabbro vary between 0.71–0.76 and 6.45–6.78 apfu. These hornblendes are tschermakite – magnesio-hornblende in composition (Figure 7) [44]. Magnesio-hornblende is developed along the tschermakite rims. The Mg# (Mg/[Mg+Fe]) of amphiboles in plagiogranites is between 0.57–0.79. The atomic proportion of Si is quite high (7.12–7.23 apfu) compared to that of the isotropic gabbro. These amphiboles exhibit magnesio-hornblende composition (Figure 7) [44]. The Mg# (Mg/[Mg+Fe]) and atomic proportion of Si for the amphiboles in MMEs vary between 0.71–0.76 and 6.75–6.87 apfu, and they have magnesio-hornblende in composition similar to that of the other rocks. (Figure 7) [44].

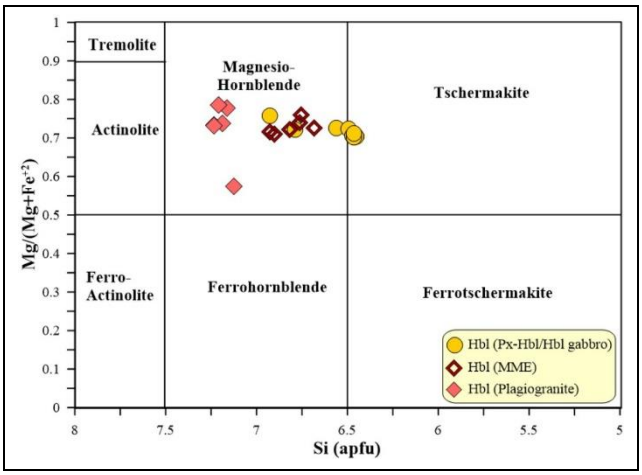

Figure 7. Classification of amphiboles in the isotropic gabbro, plagiogranite, and MME on the Mg/(Mg+Fe^{2+}) versus Si diagram [44].

4.2.3 Plagioclase

The plagioclase analysis results and calculated end members in the isotropic gabbros, plagiogranite, and MME rocks are given in Appendix C and shown in the ternary diagram in Figure 8 [45]. Different types of plagioclases (Pl I and Pl II) in the isotropic gabbros, plagiogranite, and MME present compositional differences. Pl I is in the hornblende-pyroxene gabbro, with an andesine to labradorite (Ab36–53An47–65) composition, with low CaO (7.83–10.58 wt.%) and high Na_2O (2.78–6.06 wt.%) contents compared to Pl IIs in the pyroxene-hornblende /hornblende gabbro (Figure 8a) [45]. The CaO and Na_2O contents of Pl IIs vary between 9.51–10.61 wt.% and 0.94–2.36 wt.%. Pl IIs have a relatively high anorthite content and exhibit compositions ranging from labradorite to bytownite ($Ab_{14–31}An_{69–86}$) (Figure 8a) [45]. Plagioclases (Pl IIs) in MMEs have CaO (9.58–10.49 wt.%) and Na_2O (1.86–2.82 wt.%) concentrations similar to those of pyroxene-hornblende/hornblende gabbros. They have labradorite – bytownite ($Ab_{25–35}An_{65–75}$) in composition with enriched anorthite proportion (Figure 8b) [45]. Plagioclase (Pl IIs) in plagiogranite has an andesine ($Ab_{52–61}An_{38–48}$) composition with low CaO (6.69–7.52 wt.%) and high Na_2O (5.22–5.98 wt.%) contents (Figure 8b) [45].

5 Discussion and conclusion

The ophiolite rocks around Derinkuyu are represented by isotropic gabbro and plagiogranite, which are the upper levels of the SSZ-type ophiolitic sequence in Central Anatolia. According to their textural features, the crystallization order of these rocks is plagioclase (Pl I) + clinopyroxene → plagioclase (Pl II) + hornblende. Hornblendes were developed by overprinting on the clinopyroxene. This crystallization order indicates that the mafic magma then underwent high-level fractional crystallization. Therefore, hornblende gabbros have been referred to as "high-level gabbros" in the Central Anatolia Ophiolite [6],[18]. As a secondary product, an actinolite + chlorite + epidote ± albite mineral assemblage developed, indicating that it underwent hydrothermal metamorphism at low greenschist-facies conditions on the seafloor.

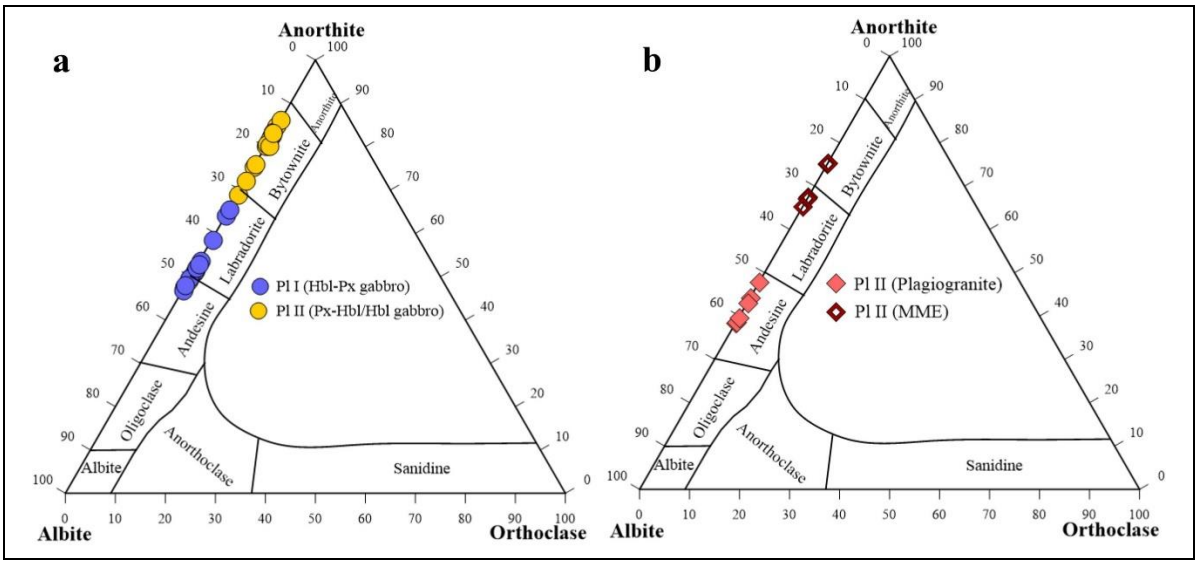

Figure 8. Ternary classification diagram showing compositional variation for plagioclases in the (a): Isotropic gabbros, and (b): Plagiogranite and MME [45].

The mineral chemistry of isotropic gabbro and plagiogranite plays a significant role in understanding the tectonic environment and crystallization conditions [5]-[12],[46]. The petrogenetic evolution and crystallization conditions of the ophiolite rocks around the Derinkuyu region are presented below under two subheadings.

5.1 Petrogenesis

Clinopyroxene and hornblende mineral chemistry results indicate a subalkaline and tholeiitic to calc-alkaline magma source in the SiO_2–Al_2O_3 (Figure 9a) [47], Ti–Ca+Na (Figure 9b) [48] and TiO_2–SiO_2 (Figure 9c) [49] diagrams. Clinopyroxene compositions reflect a tholeiitic magma source, while hornblende compositions are calc-alkaline. Clinopyroxene and hornblendes, like other those of the island arc tholeiites (IAT), have relatively high Mg# (clinopyroxene=0.73–0.84; hornblende=0.57–0.79) and low TiO_2 (clinopyroxene=0.14–0.76 wt.%; hornblende=0.52–1.73 wt.%) concentrations [5]-[13]. In the Wo–En–Fs ternary diagram (Figure 6) [42] and the Al_T–Ti tectonic discrimination diagram (Figure 9d) [50], clinopyroxenes exhibit the signature of island arc tholeiites (IAT). The formation of tholeiitic and calc-alkaline magma series on the ocean floor is controlled by the hydration of the mantle wedge, with sediment added during subduction, and by the degree of mantle depletion [1],[2]. Calc-alkaline types are suggested to have higher sediment inputs [2].

Compositional features of the hornblendes indicate the development of two different types of hornblendes, namely tschermakite and magnesio-hornblende (Figure 7). The tschermakite appears to be directly crystallized in the wet magma following crystallization of clinopyroxene + plagioclase (Pl I) [6]. Magnesio-hornblende can be said to have been formed as a secondary/late amphibole as a result of the reaction of earlier clinopyroxene with increasingly water-enriched magma [6],[46].

Plagioclase compositions, like those of clinopyroxene and hornblende, can provide clues about the crystallization process and the petrogenetic evolution of ophiolitic rocks [7],[9]-[11]. Petrographic investigations of isotropic gabbro, MME, and plagiogranite indicate the development of two distinct plagioclase types (Figure 4). Both types of calcic plagioclase appear to be magmatic. The anorthite proportion in the plagioclases of pyroxene-hornblende/hornblende gabbro ($An_{69–86}$) and MME ($An_{65–75}$) is relatively higher than those of the hornblende-pyroxene gabbro ($An_{47–65}$) (Figure 8). Similarly, high anorthite contents were determined for plagioclases in hornblende-bearing gabbroic rocks formed in SSZ-type environments [6]-[11] and island arc-related plutonic rocks [51]. It was observed that clinopyroxene transformed into hornblende in samples with higher plagioclase anorthite content. The increase in anorthite proportion in these plagioclases is related to the formation of hornblende, that is, the presence of water in the melt during crystallization [51],[52].

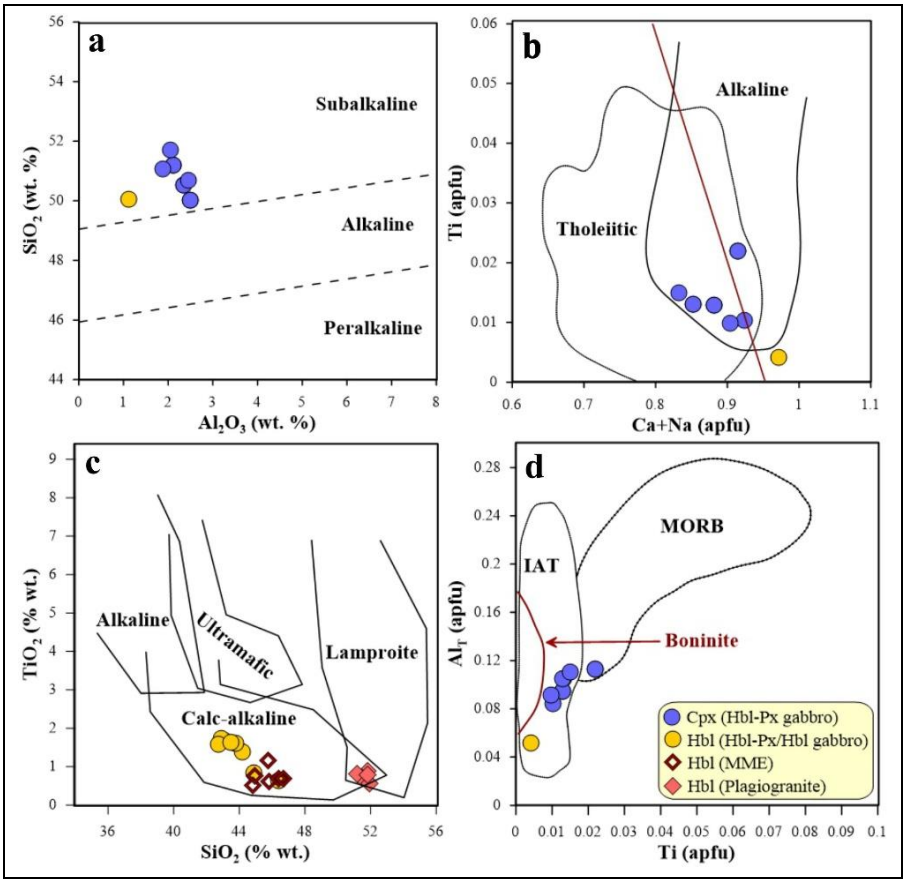

Figure 9. Plot of (a): SiO_2 versus Al_2O_3 for clinopyroxenes [47]. (b): Ti versus Ca+Na for clinopyroxenes [48]. (c): TiO_2 versus SiO_2 for hornblendes [49]. (d): Al_T versus Ti for clinopyroxenes [50] in the isotropic gabbro, plagiogranite, and MME.

The quite low anorthite proportion (An_{38-48}) of plagioclase (Pl II) in plagiogranite can indicate that it formed as a result of fractional crystallization from the pyroxene-hornblende/hornblende gabbro. The relatively low An (An_{47-65}) content of Pl I, which formed together with clinopyroxene, can be associated with a water-poor melt. Therefore, two generations of plagioclase formations derived from partly dry and hydrated melts can be mentioned. The water-poor melt can be related to the hornblende-pyroxene gabbro formation, whereas the hydrated melt produced pyroxene-hornblende/hornblende gabbro and plagiogranite. Additionally, these variations in plagioclase and hornblende compositions suggest a high-level fractional crystallization.

5.2 Crystallization conditions

Compositional differences of clinopyroxenes and hornblendes, especially their Al_2O_3 and TiO_2 contents, affect the crystallization pressure and temperature ranges [39],[40]. Elthon [53] suggested that clinopyroxenes with low-Al_2O_3 (<3 wt.%) and low-TiO_2 (<1 wt.%) contents were formed under low- to moderate-pressure (5–10 kbar) conditions. Accordingly, low-Al_2O_3 (2.50–1.11 wt.%) and TiO_2 (0.76–0.14 wt.%) concentrations in the clinopyroxenes suggest low- to moderate- P–T formation conditions for the isotropic gabbro. P–T conditions of 2.60–1.37 kbar and 1199–1186°C at 9.2-4.9 km depth were estimated for the clinopyroxenes crystallization in the hornblende-pyroxene gabbro (Appendix A) [39].

Due to calibration limitations for calc-alkali products ($Al\#={}^{IV}Al/Al_{tot}>0.21$) [40], P–T estimation for the crystallization of hornblendes in plagiogranites could not be made. The Al# of a hornblende in these rocks are high and varies between 0.27 and 0.33 (Appendix B) [40]. The calculated thermobaromeric data for hornblendes are lower than those for clinopyroxenes. Two different physicochemical conditions in the ocean crust for tschermakite and magnesio-hornblende have been identified based on amphibole mineral chemistry. Tschermakite, which indicates that it directly crystallized in the wet magma, exhibits relatively high pressure (1.95–1.78 kbar), depth (6.9–6.3 km), and temperature (864–853°C) and high H_2O content (6.8–6.7 wt.%) in the melt (Appendix B) [40]. Magnesio-hornblende developed at relatively low-pressure (1.62–1.09 kbar), depth (5.7–3.9 kbar), temperatures (844–790 °C) and high H_2O (6.1–7.2 wt.%) conditions. The physicochemical conditions predicted for clinopyroxene, tschermakite, and magnesio-hornblende indicate that fractional crystallization continued to shallow levels in the lithosphere. It can also be said that magnesio-hornblende (late amphiboles) developed as a result of the reaction of clinopyroxenes with increasingly water-enriched magma [46]. Additionally, these data are quite compatible with the thermobarometric data estimated for ophiolite gabbro of supra-subduction origin [46].

6 Acknowledgment

This work was financially supported by the Scientific Research Projects Unit of Nevşehir Hacı Bektaş Veli University (NEÜABAP21F22). We would like to thank Dr. Ahmet Orhan for his help during the field study. Anonymous reviewers are kindly appreciated for their valuable comments.

7 Author contribution statements

In the study carried out, Ayşe Orhan contributed to the formation and design of the idea, literature review, field observations and sample collection, petrographic examinations, mineral chemistry analyses, evaluation and interpretation of the data obtained, writing of the manuscript and spell checking; Musa Avni Akçe contributed to field observations and sample collection, interpretation of the results, spell checking and review of the manuscript for content.

8 Ethics committee approval and conflict of interest statement

"There is no need to obtain permission from the ethics committee for the article prepared".

"There is no conflict of interest with any person / institution in the article prepared".

9 References

[1] Pearce JA, Lippard SJ, Roberts S. *Characteristics and Tectonic Significance of Supra-Subduction Zone Ophiolites.* Editors: Kokelaar BP, Howells MF. Marginal Basin Geology, Geological Society of London, Special Publications, 16(1), 77–94, Blackwell, London, UK, 1984.

[2] Dilek Y, Furnes H, Shallo M. "Suprasubduction zone ophiolite formation along the periphery of Mesozoic Gondwana". *Gondwana Research*, 11(4), 453–475, 2007.

[3] Coleman RG, Peterman ZE. "Oceanic plagiogranite". *Journal of Geophysical Research,* 80(8), 1099–1108, 1975.

[4] Floyd PA, Yaliniz MK, Goncuoglu MC. "Geochemistry and petrogenesis of intrusive and extrusive ophiolitic plagiogranites, Central Anatolian Crystalline Complex, Turkey". *Lithos*, 42(3-4), 225–241, 1998.

[5] Yalınız MK, Göncüoğlu MC. "Clinopyroxene compositions of the isotropic gabbros from the Sarıkaraman Ophiolite: New evidence on supra-subduction zone type magma genesis in Central Anatolia". *Turkish Journal of Earth Sciences*, 8(2), 103–111, 1999.

[6] Kocak K, Isık F, Arslan M, Zedef M. "Petrological and source region characteristics of ophiolitic hornblende gabbros from the Aksaray and Kayseri regions, central Anatolian crystalline complex, Turkey". *Journal of Asian Earth Sciences*, 25(6), 883–891, 2005.

[7] Ilbeyli N. "Geochemical comparison of ultramafic-mafic cumulate rocks from the Central Anatolian Ophiolites, Turkey". *International Geology Review*, 50(9), 810–825, 2008.

[8] Bağcı U. "The geochemistry and petrology of the ophiolitic rocks from the Kahramanmaraş region, southern Turkey". *Turkish Journal of Earth Sciences*, 22(4), 536–562, 2013.

[9] Yellappa T, Tsunogae T, Chetty TRK, Santosh M. "Mineral chemistry of isotropic gabbros from the Manamedu Ophiolite Complex, Cauvery Suture Zone, southern India: Evidence for neoproterozoic suprasubduction zone tectonics". *Journal of Asian Earth Sciences*, 130, 155–165, 2016.

[10] Kadıoğlu YK, Deniz K, Koralay T, Güllü B. "Nature of the gabbro in Central Anatolia: Geological observation and spectroscopic applications, Turkey". *19th International Multidisciplinary Scientific GeoConference (SGEM 2019)*, Albena, Bulgaria, 30 June–6 July, 2019.

[11] Parlak O, Bağcı, U, Rızaoğlu T, Ionescu C, Önal G, Höck V, Kozlu H. "Petrology of ultramafic to mafic cumulate rocks from the Göksun (Kahramanmaraş) ophiolite, southeast Turkey". *Geoscience Frontiers*, 11(1), 109–128, 2020.

[12] Sato A, Imayama T, Dutta D, Kaneda Y, Watanabe S, Hasegawa T, Minami M, Wakasugi Y, Wakaki S, Yi K. "Supra-subduction zone magmatism and extreme mantle depletion in the Early Cretaceous Nidar Ophiolite Complex, NW India". *Gondwana Research*, 147, 119–136, 2025.

[13] Kadıoğlu YK, Akçe MA, Deniz K, Koralay T, Güllü B. "Orta Anadolu Gabrolarının Kökeni ve U-Pb Yöntemi ile Yaşlandırılması". Türkiye Bilimsel ve Teknik Araştırma Kurumu, Ankara, Türkiye, 116Y240, 2021.

[14] Okay AI, Tüysüz O. *Tethyan Sutures of Northern Turkey*. Editors: Durand B, Jolivet L, Horváth F, Séranne M. The Mediterranean Basins: Tertiary extension within the Alpine Orogen, Geological Society of London, Special Publications, 475–515, The Geological Society, London, UK, 1999.

[15] Lefebvre C, Peters MK, Wehrens PC, Brouwer FM, Van Roermund HLM. "Thermal history and extensional exhumation of a high-temperature crystalline complex (Hırkadağ Massif, Central Anatolia)". *Lithos*, 238, 156–173, 2015.

[16] Göncüoğlu MC, Toprak GMV, Kuşcu İ, Erler A, Olgun E. "Orta Anadolu Masifinin Batı Bölümünün Jeolojisi, Bölüm 1: Güney Kesim". Türkiye Petrolleri Anonim Ortaklığı, Ankara, Türkiye, 2909, 1991.

[17] Göncüoğlu MC, Türeli TK. "Orta Anadolu Ofiyoliti plajiyogranitlerinin petrolojisi ve jeodinamik yorumu (Aksaray-Türkiye)". *Doğa - Türk Yerbilimleri Dergisi*, 2, 195–203, 1993.

[18] Yalınız MK, Göncüoğlu MC. "General geological characteristics and distribution of the Central Anatolian Ophiolites". *Yerbilimleri*, 20, 19–30, 1998.

[19] Yaliniz MK, Floyd PA, Göncüoğlu MC. "Petrology and geotectonic significance of plagiogranite from the Sarıkaraman Ophiolite (Central Anatolia, Turkey)". *Ofioliti*, 25(1), 31–37, 2000.

[20] Yalınız MK. "A geochemical attempt to distinguish forearc and back arc ophiolites from the "supra-subduction" Central Anatolian Ophiolites (Turkey) by comparison with modern oceanic analogues". Ofioliti, 33(2), 119–129, 2008.

[21] Köksal S, Toksoy-Köksal F, Göncüoğlu MC. "Petrogenesis and geodynamics of plagiogranites from Central Turkey (Ekecikdağ/Aksaray): New geochemical and isotopic data for generation in an arc basin system within the northern branch of Neotethys". *International Journal of Earth Sciences (Geologische Rundschau)*, 106, 1181–1203, 2017.

[22] MTA. Kayseri L33b1, L33b2, L33b3 and L33b4 sheets, 1/25.000 Scaled Geological Maps. 1990.

[23] Işık F. Ekecekyeniköy-Mamasun (Aksaray) Yeşilhisar (Kayseri) Arasının Jeolojisi ve Gabroyik-Granitoyidik Kayaçların Mineralojik-Petrografik ve Jeokimyasal İncelemesi. Doktora Tezi, Selçuk Üniversitesi, Konya, Türkiye, 2000.

[24] Seymen İ. "Kaman (Kırşehir) dolayında Kırşehir Masifi'nin stratigrafisi ve metamorfizması". *Türkiye Jeoloji Kurumu Bülteni*, 24(2), 7–14, 1981.

[25] Whitney DL, Teyssier C, Dilek Y, Fayon K. "Metamorphism of the Central Anatolian Crystalline Complex, Turkey: influence of orogen-normal collision vs. wrench-dominated tectonics on *P-T-t* paths". *Journal of Metamorphic Geology*, 19(4), 411–432, 2001.

[26] Whitney DL, Teyssier C, Fayon AK, Hamilton MA, Heizler M. "Tectonic controls on metamorphism, partial melting, and intrusion: timing and duration of regional metamorphism and magmatism in the Niğde Massif. Turkey". *Tectonophysics*, 376 (1–2), 37–60, 2003.

[27] Whitney DL, Hamilton MA. "Timing of high-grade metamorphism in central Turkey and the assembly of Anatolia". *Journal of the Geological Society*, 161(5), 823–828, 2004.

[28] van Hinsbergen DJJ, Maffione M, Plunder A, Kaymakcı N, Ganerød M, Hendriks BWH, Corfu F, Gürer D, de Gelder GINO, Peters K, McPhee PJ, Brouwer FM, Advokaat EL, Vissers RLM. "Tectonic evolution and paleogeography of the Kırşehir Block and the Central Anatolian Ophiolites, Turkey". *Tectonics*, 35(4), 983–1014, 2016.

[29] Akıman O, Erler A, Göncüoğlu MC, Güleç N, Geven A, Türeli TK, Kadıoğlu YK. "Geochemical characteristics of granitoids along the western margin of the Central Anatolian Crystalline Complex and their tectonic implications". *Geological Journal*, 28(3-4), 371–382, 1993.

[30] Aydın NS, Malpas J, Göncüoglu MC, Erler A. "A review of the nature of magmatism in Central Anatolia during the Mesozoic post collisional period". *International Geology Review*, 43(8), 695–710, 2001.

[31] Ilbeyli N, Pearce JA, Thirlwall MF, Mitchell JG. "Petrogenesis of collision related plutonic in Central Anatolia, Turkey". *Lithos*, 72(3-4), 163–182, 2004.

[32] Kadıoğlu YK, Dilek Y, Foland KA. *Slab Break-of and Syncollisional Origin of the Late Cretaceous magmatism in the Central Anatolian crystalline complex, Turkey.* Editors: Dilek Y, Pavlides S. Postcollisional Tectonics and Magmatism in the Mediterranean Region and Asia, Geological Society of America, Special Paper, 381–415, Boulder, CO, USA, 2006.

[33] Köksal S, Göncüoğlu MC. "Sr and Nd isotopic characteristics of some S-, I and A-type granitoids from Central Anatolia". *Turkish Journal of Earth Sciences*, 17(1), 11–127, 2008.

[34] Orhan A, Demirbilek M. "Kapadokya bölgesi (Nevşehir, Orta Anadolu) kalk-alkalen ve alkalen plütonik/ subvolkanik kayaçların petrografik ve jeokimyasal özellikleri". *Türkiye Jeoloji Bülteni*, 61(1), 23–50, 2018.

[35] Divilioğlu E, Orhan A. "Avanos (Nevşehir, Orta Anadolu) yöresindeki Geç Kretase yaşlı alkalen plütonik ve subvolkanik kayaçların jeokimyası, mineral kimyası ve kristallenme koşulları". *Türkiye Jeoloji Bülteni*, 66(2), 159–188, 2023.

[36] Köksal S, Romer RL, Göncüoglu MC, Toksoy-Köksal F. "Timing of postcollisional H-type to A-type granitic magmatism: U-Pb titanite ages from the Alpine central Anatolian granitoids (Turkey)". *International Journal of Earth Sciences (Geologische Rundschau)*, 93(6), 974–989, 2004.

[37] Boztuğ D, Tichomirowa M, Bombach K. "^{207}Pb–^{206}Pb single-zircon evaporation ages of some granitoid rocks reveal continent-oceanic island arc collision during the Cretaceous geodynamic evolution of the central Anatolian crust, Turkey". *Journal of Asian Earth Sciences*, 31(1), 71–86, 2007.

[38] Orhan A, Akçe MA, Divilioğlu E. "Nevşehir-Niğde Bölgesi Plütonik Kayaçların Mineral Bileşimleri ve Kristalizasyon Koşullarının (P-T) Araştırılması". NEÜBAP Bilimsel Araştırma Projesi, Nevşehir, Türkiye, ABAP21F22, 2022.
[39] Wang X, Hou T, Wang M, Zhang C, Zhang Z, Pan R, Marxer F, Zhang H. "A new clinopyroxene thermobarometer for mafic to intermediate magmatic systems". *European Journal of Mineralogy*, 33(5), 621–637, 2021.
[40] Ridolfi F, Renzulli A, Puerini M. "Stability and chemical equilibrium of amphibole in calc-alkaline magmas: an overview, new thermobarometric formulations and application to subduction-related volcanoes". *Contributions to Mineralogy and Petrology*, 160(1), 45–66, 2010.
[41] Streckeisen A. "Classification and nomenclature of plutonic rocks recommendations of the IUGS subcommission on the systematics of igneous rocks". *Geologische Rundschau*, 63(2), 773–786, 1974.
[42] Morimoto N. "Nomenclature of pyroxenes". *Mineralogy and Petrology*, 39(1), 55–76, 1988.
[43] Burns LE. "The Border Ranges ultramafic and mafic complex, south central Alaska: cumulate fractionates of island arcs volcanics". *Canadian Journal of Earth Sciences*, 22(7), 1020–1038, 1985.
[44] Leake BE, Woolley AR, Arps CES, Birch WD, Gilbert MC, Grice JD, Hawthorne FC, Kato A, Kisch HJ, Krivovichev VG, Linthout K, Laird J, Mandarino JA, Maresch WV, Nickel EH, Rock NMS, Schumacher JC, Smith DC, Stephenson NCN, Ungaretti L, Whittaker EJW, Youzhi G. "Nomenclature of amphiboles: Report of the subcommittee on amphiboles of the International Mineralogical Association, Commission on New Minerals and Mineral Names". *The Canadian Mineralogist*, 35(1), 219–246, 1997.
[45] Deer WA, Howie RA, Zussman J. *An Introduction to Rock Forming Minerals*. 1st ed. New York, USA, John Wiley and Sons, 1966.
[46] Ustalić S, Nemec O, Milovská S, Putiš M, Babajić E, Kurylo E, Ružička P. "Amphibole group minerals in the Ozren Massif Ophiolites of Bosnia and Herzegovina as petrogenetic indicators". *Minerals*, 14(3), 239, 2024.
[47] Le Bas MJ. "The role of aluminium in igneous clinopyroxenes with relation to their parentage". *American Journal of Science*, 260(4), 267–288, 1962.
[48] Leterrier J, Maury RC, Thonon P, Girard D, Marchal M. "Clinopyroxene composition as a method of identification of the magmatic affinities of paleovolcanic series". *Earth and Planetary Science Letters*, 59(1), 139–154, 1982.
[49] Droop GTR, "A general equation for estimating Fe^{3+} concentrations in ferromagnesian silicates and oxides from microprobe analyses, using stoichiometric criteria". *Mineralogical Magazine*, 51(361) 431–435, 1987.
[50] Beccaluva L, Macciotta G, Piccardo GB, Zeda O. "Clinopyroxene composition of ophiolite basalts as petrogenetic indicator". *Chemical Geology*, 77(3-4), 165–182, 1989.
[51] Arculus RJ, Wills KJA. "The petrology of plutonic blocks and inclusions from the Lesser Antilles island arc". *Journal of Petrology,* 21(4), 743–799, 1980.
[52] Helz RT. "Phase relations of basalt in their melting range at P_{H_2O}=5 kb as a function of oxygen fugacity: Part I. mafic phases". *Journal of Petrology*, 14(2), 249–302, 1973.
[53] Elthon D. "Petrology of the gabbroic rocks from the Mid-Cayman Rise spreading center". *Journal of Geophysical Research*, 92(B1), 658–682, 1987.

Appendix A

Representative electron microprobe analysis results of clinopyroxene (wt. %) in the isotropic gabbro.

Sample no	TK8-1-1-1	TK8-1-1-2	TK8-1-1-3	TK8-2-1-1	TK8-2-1-2	TK8-2-1-3	TK8-2-1-4	TK8-2-1-5	TK8-2-1-7	CT-4-2-1-3
SiO_2	51.21	50.52	50.01	51.21	50.52	50.01	50.69	51.06	51.71	50.06
TiO_2	0.45	0.45	0.76	0.45	0.45	0.76	0.52	0.36	0.35	0.14
Al_2O_3	2.11	2.34	2.50	2.11	2.34	2.50	2.46	1.88	2.06	1.11
Cr_2O_3	0.10	0.12	0.03	0.10	0.12	0.03	0.11	0.06	0.11	0.00
FeO	7.87	8.06	9.38	7.87	8.06	9.38	8.92	7.52	7.21	8.85
MnO	0.00	0.00	0.00	0.00	0.00	0.00	0.00	0.00	0.00	0.00
MgO	14.43	14.67	12.77	14.43	14.67	12.77	14.62	13.99	14.40	12.67
CaO	21.12	20.27	21.48	21.12	20.27	21.48	19.88	22.06	21.94	22.42
Na_2O	0.32	0.29	0.42	0.32	0.29	0.42	0.32	0.32	0.23	0.39
K_2O	0.00	0.00	0.00	0.00	0.00	0.00	0.00	0.01	0.00	0.01
Total	97.61	96.71	97.34	97.61	96.72	97.34	97.52	97.25	98.02	95.64
Si	1.943	1.932	1.919	1.943	1.932	1.919	1.927	1.945	1.952	1.963
Ti	0.013	0.013	0.022	0.013	0.013	0.022	0.015	0.010	0.010	0.004
Al	0.094	0.105	0.113	0.094	0.105	0.113	0.110	0.084	0.092	0.051
Cr	0.003	0.004	0.001	0.003	0.004	0.001	0.003	0.002	0.003	0.000
Fe^{2+}	0.250	0.258	0.301	0.250	0.258	0.301	0.284	0.240	0.228	0.290
Mn	0.000	0.000	0.000	0.000	0.000	0.000	0.000	0.000	0.000	0.000
Mg	0.816	0.837	0.730	0.816	0.837	0.730	0.828	0.795	0.811	0.741

Appendix A. Continued.

Sample no	TK8-1-1-1	TK8-1-1-2	TK8-1-1-3	TK8-2-1-1	TK8-2-1-2	TK8-2-1-3	TK8-2-1-4	TK8-2-1-5	TK8-2-1-7	CT-4-2-1-3
Ca	0.858	0.830	0.883	0.858	0.830	0.883	0.809	0.900	0.887	0.942
Na	0.024	0.022	0.031	0.024	0.022	0.031	0.023	0.024	0.017	0.030
K	0.000	0.000	0.000	0.000	0.000	0.000	0.000	0.000	0.000	0.000
Total	4.000	4.000	4.000	4.000	4.000	4.000	4.000	4.000	4.000	4.022
Wo	44.08	42.71	45.45	44.08	42.68	45.41	41.63	45.98	45.67	47.07
En	41.91	43.03	37.60	41.91	43.00	37.56	42.61	40.59	41.72	37.01
Fs	12.81	13.14	15.34	12.81	13.21	15.43	14.55	12.21	11.72	14.43
Mg#	0.78	0.84	0.80	0.78	0.78	0.73	0.76	0.79	0.78	0.77
T (°C)	1194	1197	-	1194	1197	-	-	1186	1199	-
P (kbar)	1.62	1.37	-	2.57	2.26	-	-	2.12	2.60	-
Depth (km)	5.7	4.9		9.1	8.0		-	7.5	9.2	-

Appendix B

Representative electron microprobe analyses results of amphiboles (wt. %) in the isotropic gabbro. plagiogranite and MME.

Rock type	Isotropic gabbro				Plagiogranite					MME			
Sample no	Mg-Hbl	Tsch	Tsch	Mg-Hbl	Mg-Hbl	Mg-Hbl	Mg-Hbl	Mg-Hbl	Mg-Hbl	Mg-Hbl	Mg-Hbl	Mg-Hbl	Mg-Hbl
	CT-4-1-1-1	CT-4-1-1-2	CT-4-1-1-6	CT-4-2-1-1	CT-17-1-1-1	CT-17-1-1-2	CT-17-1-1-3	CT-17-1-1-4	CT-17-1-1-5	CT-14-1-1-1	CT-14-1-1-2	CT-14-1-1-4	CT-14-1-2-2
SiO_2	44.18	43.75	43.46	46.40	51.83	51.82	51.49	51.17	51.93	45.81	46.41	46.71	44.95
TiO_2	1.38	1.61	1.63	1.63	0.88	0.61	0.72	0.81	0.57	0.60	0.68	0.70	0.77
Al_2O_3	8.48	8.85	9.18	7.31	6.95	7.33	7.32	7.33	6.67	7.86	6.94	7.58	8.43
FeO	16.61	16.87	16.65	14.89	15.75	15.67	15.55	16.79	15.83	15.99	15.79	15.74	16.25
MnO	0.00	0.00	0.00	0.00	0.00	0.00	0.00	0.00	0.00	0.00	0.00	0.00	0.00
MgO	12.35	12.11	12.01	13.62	12.94	13.44	13.05	12.69	13.55	12.94	12.60	12.51	12.32
CaO	11.34	11.24	11.35	11.62	10.44	10.47	10.59	9.84	10.38	11.42	11.30	11.33	11.45
Na_2O	1.46	1.51	1.55	0.88	0.74	0.81	0.83	0.78	0.74	0.98	0.93	0.98	1.05
K_2O	0.12	0.10	0.15	0.17	0.12	0.13	0.11	0.11	0.10	0.18	0.16	0.17	0.20
Cr_2O_3	0.05	0.05	0.06	0.02	0.00	0.01	0.01	0.00	0.01	0.01	0.00	0.02	0.01
Total	95.98	96.09	96.04	96.53	99.64	100.28	99.67	99.52	99.76	95.80	95.80	95.73	95.41
Si	6.560	6.493	6.466	6.777	7.235	7.163	7.188	7.124	7.208	6.753	6.868	6.901	6.684
^{IV}Al	1.440	1.507	1.534	1.223	0.765	0.837	0.812	0.876	0.792	1.247	1.132	1.099	1.316
Ti	0.000	0.000	0.000	0.000	0.000	0.000	0.000	0.000	0.000	0.000	0.000	0.000	0.000
Tsite	8.00	8.00	8.00	8.00	8.00	8.00	8.00	8.00	8.00	8.00	8.00	8.00	8.00
^{VI}Al	0.043	0.041	0.076	0.035	0.377	0.356	0.393	0.326	0.298	0.118	0.079	0.221	0.161
Ti	0.154	0.180	0.182	0.179	0.092	0.063	0.076	0.084	0.059	0.067	0.087	0.078	0.086
Cr	0.006	0.006	0.007	0.002	0.000	0.001	0.001	0.000	0.001	0.001	0.000	0.002	0.001
Fe^{3+}	1.029	1.073	0.995	0.911	0.860	1.015	0.853	0.000	1.070	1.072	0.801	0.819	0.993
Mg	2.734	2.679	2.664	2.965	2.692	2.769	2.715	2.635	2.804	2.842	2.781	2.755	2.731
Fe^{2+}	1.033	1.021	1.077	0.908	0.979	0.796	0.962	1.955	0.767	0.899	1.153	1.126	1.028
Mn	0.000	0.000	0.000	0.000	0.000	0.000	0.000	0.000	0.000	0.000	0.000	0.000	0.000
Csite	5.00	5.00	5.00	5.000	5.000	5.000	5.000	5.000	5.000	5.000	5.000	5.000	5.000
Ca	1.804	1.787	1.809	1.818	1.561	1.550	1.585	1.467	1.543	1.804	1.791	1.794	1.824
Na	0.196	0.213	0.191	0.182	0.200	0.217	0.224	0.210	0.200	0.196	0.209	0.206	0.176

Appendix B. Continued.

Rock type	Isotropic gabbro				Plagiogranite					MME			
Bsite	2.00	2.00	2.00	2.00	1.761	1.766	1.809	1.677	1.743	2.000	2.000	2.000	2.000
Na	0.225	0.222	0.255	0.067	0.000	0.000	0.000	0.000	0.000	0.084	0.057	0.076	0.127
K	0.023	0.018	0.028	0.031	0.022	0.024	0.020	0.020	0.018	0.034	0.030	0.032	0.037
Asite	0.25	0.24	0.28	0.1	0.02	0.02	0.02	0.02	0.02	0.12	0.088	0.11	0.16
(B)(Ca+Na)	2.000	2.000	2.000	2.000	2.000	2.000	1.807	2.000	2.000	2.000	2.000	2.000	2.000
$Mg/Mg+Fe^{2+}$	0.726	0.724	0.712	0.766	0.733	0.777	0.738	0.574	0.785	0.760	0.707	0.710	0.726
Al_T	1.483	1.548	1.610	1.260	1.143	1.194	1.205	1.203	1.090	1.366	1.211	1.319	1.477
Al#	0.03	0.03	0.05	0.03	0.33	0.30	0.33	0.27	0.27	0.09	0.06	0.15	0.11
T (°C)	844	853	864	811	-	-	-	-	-	809	790	793	825
Uncertainty (σest)	22	22	22	22	-	-	-	-	-	22	22	22	22
P (MPa)	162	178	195	117	-	-	-	-	-	137	109	127	161
Uncertainty (max)	18	20	21	13	-	-	-	-	-	15	12	14	18
Ocean depth (km)	5.7	6.3	6.9	4.1	-	-	-	-	-	4.8	3.9	4.5	5.7
H_2O_{melt} (wt.%)	6.5	6.7	6.8	6.1						6.8	6.3	7.0	7.2
Uncertainty*	0.4	1.0	1.0	0.4						0.4	0.4	0.4	0.4

Appendix C

Representative electron microprobe analyses results of plagioclase (wt. %) in the isotropic gabbro. plagiogranite and MME.

Rock type	Isotropic gabbro					Plagiogranite				MME		
Sample no	TK-8-1-1 (Pl I)	TK-8-1-2 (Pl I)	TK-8-2-1 (Pl I)	CT-4-1-1 (Pl II)	CT-4-2-1 (Pl II)	CT-4-2-9 (Pl I)	CT-17-1-1 (Pl II)	CT-17-1-3 (Pl II)	CT-17-1-6 (Pl II)	CT-14-1-1 (Pl II)	CT-14-1-3 (Pl II)	CT-14-2-2 (Pl II)
SiO_2	56.89	53.92	54.25	53.17	52.50	51.52	56.32	58.22	56.09	52.03	52.69	52.32
TiO_2	0.07	0.07	0.05	0.03	0.00	0.00	0.00	0.00	0.01	0.03	0.01	0.01
Al_2O_3	29.78	32.00	32.12	34.74	35.71	29.86	30.35	28.70	30.15	33.76	33.95	34.62
FeO	0.42	0.48	0.42	0.17	0.18	0.32	0.07	0.04	0.10	0.24	0.24	0.16
MnO	0.00	0.00	0.00	0.00	0.00	0.00	0.00	0.00	0.00	0.00	0.00	0.00
MgO	0.03	0.03	0.03	0.01	0.01	0.07	0.00	0.00	0.02	0.04	0.03	0.00
CaO	7.83	8.57	9.55	10.09	10.61	10.58	7.93	6.73	7.32	9.85	9.58	10.25
Na_2O	4.89	4.44	2.78	1.76	0.94	6.06	4.79	5.98	5.36	2.62	2.82	1.86
K_2O	0.04	0.05	0.03	0.01	0.00	0.04	0.03	0.04	0.06	0.01	0.02	0.01
Total	99.96	99.54	99.24	99.98	99.97	98.46	99.48	99.71	99.10	98.58	99.33	99.23
Si	2.577	2.451	2.507	2.450	2.431	2.337	2.561	2.624	2.548	2.415	2.423	2.426
Al	1.590	1.714	1.749	1.886	1.949	1.596	1.626	1.525	1.614	1.846	1.840	1.891
Ti	0.002	0.002	0.002	0.001	0.000	0.000	0.000	0.000	0.000	0.001	0.000	0.000
Fe	0.016	0.018	0.016	0.007	0.007	0.012	0.003	0.002	0.004	0.009	0.009	0.006
Mn	0.000	0.000	0.000	0.000	0.000	0.000	0.000	0.000	0.000	0.000	0.000	0.000

Appendix C. Continued.

Rock type	**Isotropic gabbro**					**Plagiogranite**				**MME**		
Mg	0.002	0.002	0.002	0.001	0.001	0.005	0.000	0.000	0.001	0.003	0.002	0.000
Ca	0.380	0.417	0.473	0.498	0.527	0.514	0.386	0.325	0.356	0.490	0.472	0.509
Na	0.430	0.391	0.249	0.158	0.085	0.533	0.422	0.522	0.473	0.236	0.252	0.167
K	0.002	0.003	0.002	0.001	0.000	0.002	0.002	0.002	0.003	0.001	0.001	0.001
Total	5.000	5.000	5.000	5.000	5.000	5.000	5.000	5.000	5.000	5.000	5.000	5.000
Or	0.31	0.38	0.27	0.12	0.04	0.24	0.24	0.27	0.41	0.11	0.19	0.10
Ab	52.89	48.22	34.43	24.01	13.86	50.78	52.07	61.48	56.78	32.49	34.71	24.65
An	46.80	51.40	65.30	75.88	86.10	48.98	47.69	38.25	42.81	67.40	65.10	75.25